

*Flexible ZIFs – probing guest-induced flexibility with
CO₂, N₂ and Ar adsorption*

*Antonio Noguera-Díaz^{a,*l}, Jhonny Villarroel-Rocha^b, Valeska P Ting^c, Nuno Bimbo^d,
Karim Sapag^b and Timothy J Mays^{a,*}*

^aDepartment of Chemical Engineering, University of Bath, Claverton Down, Bath, BA2 7AY, United Kingdom.

^bLaboratorio de Sólidos Porosos, INFAP, CONICET, Universidad Nacional de San Luis, Ejército de los Andes 950, CP:5700, San Luis, Argentina.

^cDepartment of Mechanical Engineering, University of Bristol, Bristol BS8 1TR, Bristol, United Kingdom

^dDepartment of Engineering, Lancaster University, Bailrigg, Lancaster, LA1 4YW, United Kingdom

^lPresent address: VTS Schwedt GmbH, Brandenburg, Germany

*Corresponding author 1: Antonio Noguera-Díaz, VTS Schwedt GmbH, Brandenburg, Germany. Tel.: +49 1520 3709484. E-mail address: a.j.noguera@hotmail.com

*Corresponding author 2: Timothy J Mays, Department of Chemical Engineering, University of Bath, Claverton Down, Bath, BA2 7AY, United Kingdom. Tel.: +44 (0) 1225 386528. E-mail address: t.j.mays@bath.ac.uk

Abstract

Background: The effect of framework topology on the guest-induced flexibility of several crystalline zeolitic imidazolate frameworks (ZIF-7, ZIF-9, ZIF-11 and ZIF-12) was investigated via analysis of experimental N₂, CO₂ and Ar isotherms at 77 K (N₂ and Ar) and 273 K (CO₂) for gas pressures up to 0.13 MPa.

Results: The experimental isotherms were analysed in order to investigate structural flexibility of these materials using gases with kinetic diameters equal to or larger than the diameters of their static pore apertures. The results of gas sorption measurements indicate guest-induced phase changes for ZIF-7 and ZIF-9 (SOD topologies). ZIF-12 (RHO topology) also shows uptake for gases, despite its pore limiting diameter being smaller than the kinetic diameters of the adsorbed molecules.

Conclusions: This work highlights the ability of ZIFs with different framework topologies to change their structure and increase their pore aperture upon interaction with certain gases. These findings are key in the development of more selective ZIF-based materials for important industrial applications including low-energy gas separations, catalytic nanoreactors and sensor technology.

Keywords: gas adsorption, MOF, ZIF, flexibility, breathing structure, nanomaterials.

1. Introduction

Metal-organic frameworks (MOFs) have been heavily researched as adsorbents in a variety of applications that include gas storage, gas separation and catalysis. This is mainly due to their high accessible surface areas (in comparison to materials such as activated carbons, zeolites and porous polymers), permanent porosities and tuneable structures (1-3). MOFs are crystalline materials composed of organic linkers connecting metal clusters, with open channels that range in size from the micropore (<

2 nm diameter) to the mesopore scales (2-50 nm in diameter) (4). Due to their crystalline structures, MOFs can be easily characterised using X-ray diffraction techniques, making their identification relatively straightforward (2, 3).

ZIFs (zeolitic imidazolate frameworks) are a subclass of MOFs that have structures resembling those of zeolites (5, 6). They incorporate imidazoles as organic linkers, connected with metal clusters (e.g., Zn, Co), forming a 145° angle, similar to the 145° Si-O-Si angle found in zeolites (5). Almost 30 different zeolite topologies have also been reported for ZIFs (7, 8). Materials with certain topologies, such as SOD and RHO, have shown extraordinary thermal and chemical stability, being even able to resist boiling aqueous alkaline solutions and organic solvents (5, 9). ZIF materials with SOD topologies are composed of truncated beta cages (cuboctahedrons), comprising windows of four- and six-membered rings having 24 Co or Zn atoms per unit cell, with a cubic arrangement of interconnected beta cages (5, 7, 8, 10). ZIF materials with RHO topologies consist of alpha cages, with windows comprising four-, six- and eight-membered rings, having 48 Zn or Co atoms per unit cell. Each alpha cage is connected to the six neighbouring alpha cages through polyhedral units comprised of double eight-membered rings (known as D8R) (5, 7, 8, 10). Recently, it was shown that ZIFs could retain their chemical configuration, bonding and porosity when melted, showing that these MOFs can also exist in the liquid state (11).

ZIFs have been the subject of much attention due to the flexible behaviour of the framework structure, which can be induced by either guest molecule adsorption, temperature or pressure changes. Flexible MOFs are interesting in various areas, with the most prominent being gas separation and sensor technology. ZIF-8 has shown

notable framework flexibility under very high pressure with adsorption of guest molecules, which has been associated with the rotation of the imidazole linkers (12). ZIF-7 (SOD topology) has also shown a sorbate-induced gate-opening phenomenon, which was first showed by Aguado et al., with the adsorption of CO₂ (13). This gate-opening phenomena involved a narrow-to-large pore phase transition, which was then further confirmed with C2-C4 alkane/alkene adsorption (14, 15). This structural change was afterwards studied using high-resolution neutron diffraction, and the analysis showed the importance of the rotation of the benzimidazole linkers (16). The pore windows of ZIF-7 are approximately 0.29 nm in the small pore configuration and can allow molecules of 0.52 nm in diameter when they are in the large-pore phase (17). CO₂ is primarily adsorbed in two small cavities formed by the benzimidazole linkers in the six-membered rings of zinc atoms, which rotate upon CO₂ adsorption and open the cavities to accommodate further CO₂ molecules (16). These phase transitions were investigated, and at least three different phases for ZIF-7 were identified (18). The behaviour of ZIF-7 has also been recently suggested to be more complex than initially thought, as temperature can also drive phase changes in the structure, with ZIF-7 undergoing a phase change from narrow pore to large pore at 973 K in vacuum or at 773 K in CO₂ or N₂ (19). Interestingly, in this study ZIF-7 also showed a second step at higher CO₂ pressures at low temperatures (i.e. at 196 K, 206 K and 263 K) which doubled the CO₂ loading (19). This second step was reported in the paper to be associated with the rearrangement of CO₂ molecules in the pores of the large-pore phase. More recently, CH₄ was also shown induce gate-opening in ZIF-7, with the transition estimated at 1245 kPa for CH₄ and 78 kPa for CO₂, both at 303 K (17). This reversible transition was also assigned to the flexibility of the benzimidazole linkers, which enable a large-pore phase that can allow molecules of 0.52 nm diameter to enter

the main cavities. In addition to CO₂ and CH₄, other molecules have been shown to induce a phase-change in ZIFs - in our past work we have shown this effect for H₂ adsorption in ZIF-7 and ZIF-9 (20), and other reports showed phase changes upon adsorption of ethane, ethylene, propane, propene, butane and butane in ZIF-7 (15, 21). Other ZIF materials have been investigated for the phase transition seen in ZIF-7 using CO₂ adsorption, such as ZIF-11, ZIF-93 and ZIF-94, a group of ZIFs that combine RHO and SOD topology, but the only ZIF material that showed a phase transition was ZIF-7 (22). In our previous work, we showed that ZIF-9 (SOD topology), which only differs from ZIF-7 in the nature of the metal cluster (Co rather than Zn), also showed the same features as ZIF-7 upon the adsorption of hydrogen at 77 K and at 1 MPa (20). To our knowledge, no CO₂ adsorption has been measured on this material. There is much interest in further exploring the phenomena and defining the flexible responses in order to apply them in specific technology fields such as in gas separations, microsensors, micromechanical devices, and nanomedicine or catalytic nanoreactors (23).

In this paper, we investigate CO₂, N₂ and Ar adsorption in ZIF-7 (SOD), ZIF-9 (SOD), ZIF-11 (RHO) and ZIF-12 (RHO), with the goal of probing the flexible features in these structures. ZIF-7 and ZIF-9 share the same topology (SOD), but are made of different metal centres (Zn and Co), just as ZIF-11 and ZIF-12 share the same topology (RHO), but contain different metals (also Zn and Co).

2. Experimental

The materials were synthesised according to methodologies reported in the literature, using methanol (ZIF-12) and ethanol (ZIF-7, ZIF-9 and ZIF-11) but with their syntheses scaled up to ensure that enough material was available for the experimental tests (7).

Powder XRD measurements were run on a Bruker D8 Advance Diffractometer (Bruker, Billerica, US) using Cu-K α radiation, $\lambda = 0.154184$ nm, a lynxeye detector at 40 kV and 40 mA over a 2θ range of 0 to 40 $^\circ$ with a step size of 0.041 $^\circ$ s $^{-1}$ to confirm phase purity. Measurements were done in flat plate mode at 298 K on wet samples (methanol for ZIF-12 and ethanol for ZIF-7, ZIF-9 and ZIF-11), with the solvents used in several cycles to wash the samples. Experimental powder XRD spectra were compared against the original CIF files obtained from the Cambridge Crystallographic Database as well as literature publications in order to ensure the correct synthesis of the materials, details of which can be found in our previous work (7, 20). The XRD spectra for ZIF-7 and ZIF-9 are shown in Figure 1 and the XRD spectra for ZIF-11 and ZIF-12 are shown in Figure 2. Differences in the calculated and experimental XRD patterns have been attributed to the effect of different solvent washing cycles on the XRD spectra (7).

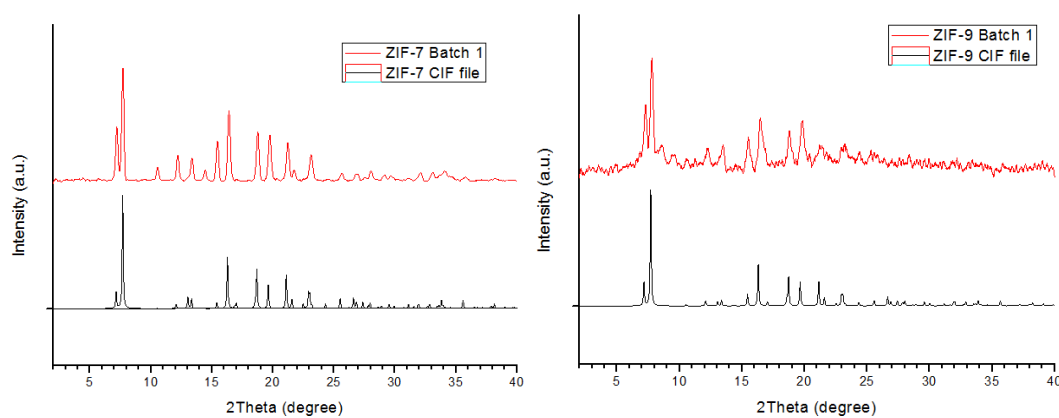


Figure 1. Powder X-ray Diffraction spectra of ZIF-7 (left) and ZIF-9 (right). The red spectrum is from the synthesized material and the black spectrum is generated from the CIF file from He et al. (7) for ZIF-7 and Li et al. for ZIF-9 (24). Spectra have been offset in the y-axis for clarity.

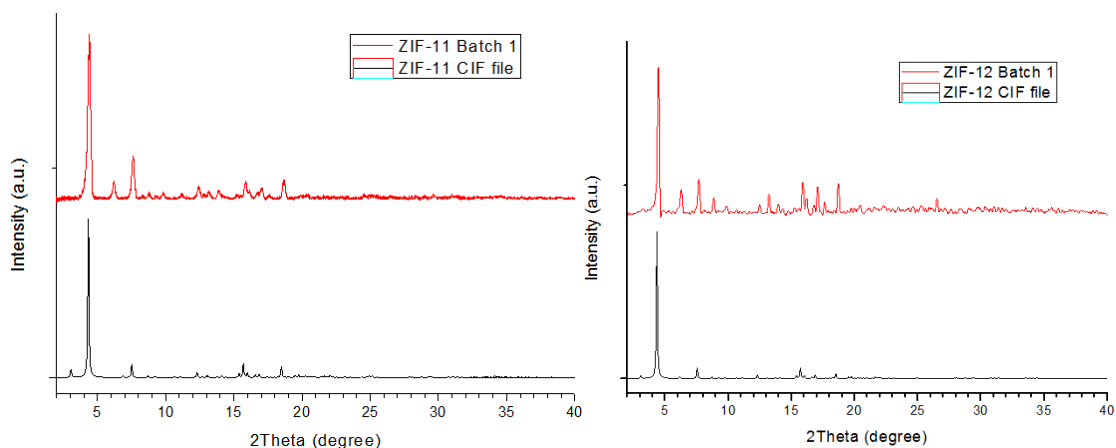


Figure 2. Powder X-ray Diffraction spectra of ZIF-11 (left) and ZIF-12 (right). The red spectrum is from the synthesized material and the black spectrum is generated from the CIF file from He et al. for both ZIF-11 and ZIF-12 (7). Spectra have been offset in the y-axis for clarity.

We previously investigated the stability of the synthesized materials in order to determine degassing conditions (20). These were performed on a Setaram TGA 92 16.18 (Setaram, Caluire, France), with the materials heated at 5 K min^{-1} from 293 to 873 K in flowing, dry N_2 at 1 bar. Degassing temperatures were thus determined to be 473, 498, 523 and 573 K for ZIF-7, ZIF-9, ZIF-11 and ZIF-12 respectively (see the Supporting Information for a summary of the data). For adsorption tests using N_2 at 77 K, Ar at 77 K and CO_2 at 273 K, an Autosorb 1-MP (Quantachrome Instruments, Boynton Beach, Florida, USA) and a Micromeritics ASAP 2020 (Micromeritics Instrument Corporation, Georgia, USA) were used. The gas sorption analyses were performed on ~ 100 mg samples degassed under dynamic high vacuum (10^{-7} mbar) at the temperatures noted above, prior to analysis. It should be noted that the Ar characterisation was done at 77 K, whereas the IUPAC methodology for characterisation of porous materials recommends that Ar analysis should be done at 87 K (25). This is due to the sensitivity of the Ar cross-sectional area to the temperature,

as at 77 K the Ar monolayer is highly dependent on the structure of the adsorbent surface (25). The main aim of the work was to probe the structure of the ZIFs with different gases, investigating the interaction of the adsorbent with different probe gases. Unlike nitrogen, Ar has no quadrupole moment, is less reactive and interacts differently with adsorbents. As no significant adsorption occurred, and the BET areas for the materials given in SI calculated from Ar are to be taken with this in mind, the fact that the Ar adsorption was done at 77 K is less relevant.

To calculate BET surface areas, the standard method consistent with the 2015 IUPAC Technical Report and BS ISO 9277:2010, (which uses the consistency criteria reported by Rouquerol) was applied (25-27). To obtain the micropore volume and total pore volume of the materials, Dubinin-Radushkevich (DR) and Gurvich methodologies were used, respectively (28, 29).

3. Results and discussion

A summary of the different pore diameters of the different materials and kinetic diameters of the different molecules involved in the analyses are shown in Table 1:

Table 1. Summary of pore size and kinetic diameters of the different materials and molecules.

Name:	Pore size (ZIFs) or kinetic diameter (nm):	Reference:
ZIF-7, ZIF-9	0.29	(7)
ZIF-11	0.30	(7)

ZIF-12	0.32	(30)
CO ₂	0.33	(31)
Ar	0.354	(31)
N ₂	0.364	(31)
Methanol	0.36	(32)
Ethanol	0.45	(32)

Adsorption isotherms with CO₂, N₂ and Ar are shown for ZIF-7 (SOD), ZIF-9 (SOD), ZIF-11 (RHO) and ZIF-12 (RHO) in Figures 3 to 6.

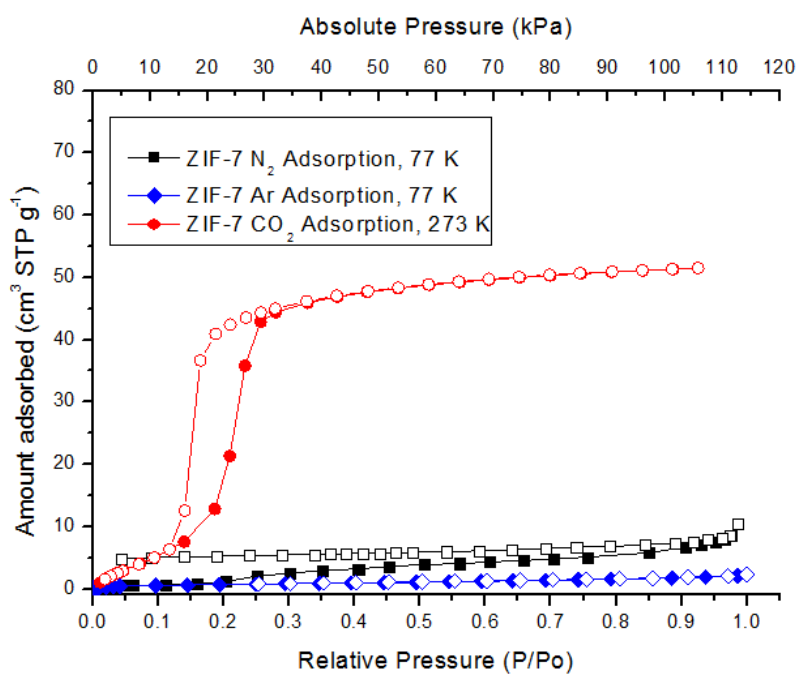


Figure 3. Adsorption isotherms of N₂ at 77 K, Ar at 77 K and CO₂ at 273 K on ZIF-7. Relative pressure refers to N₂ and Ar while the absolute pressure axis refers to the CO₂ isotherm. Open symbols indicate desorption points.

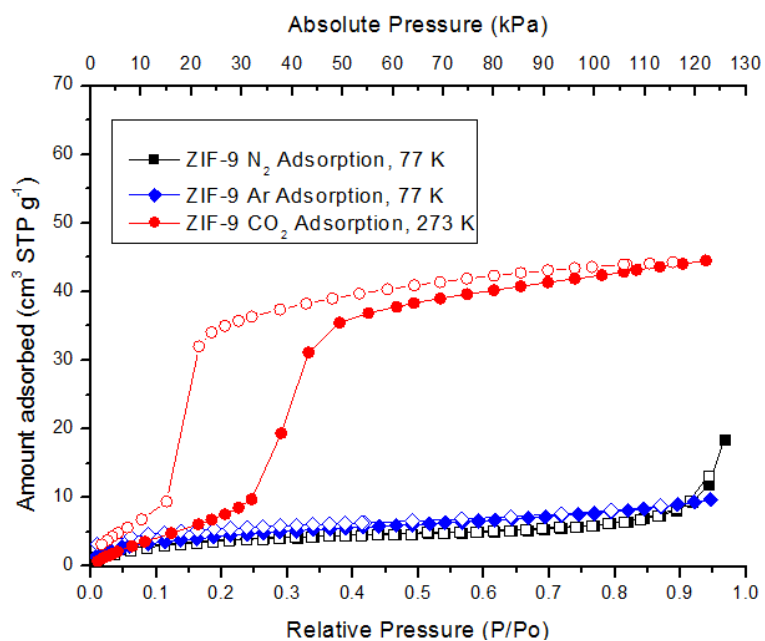


Figure 4. Adsorption isotherms of N₂ at 77 K, Ar at 77 K and CO₂ at 273 K on ZIF-9. Relative pressure refers to N₂ and Ar while the absolute pressure axis refers to the CO₂ isotherm. Open symbols indicate desorption points.

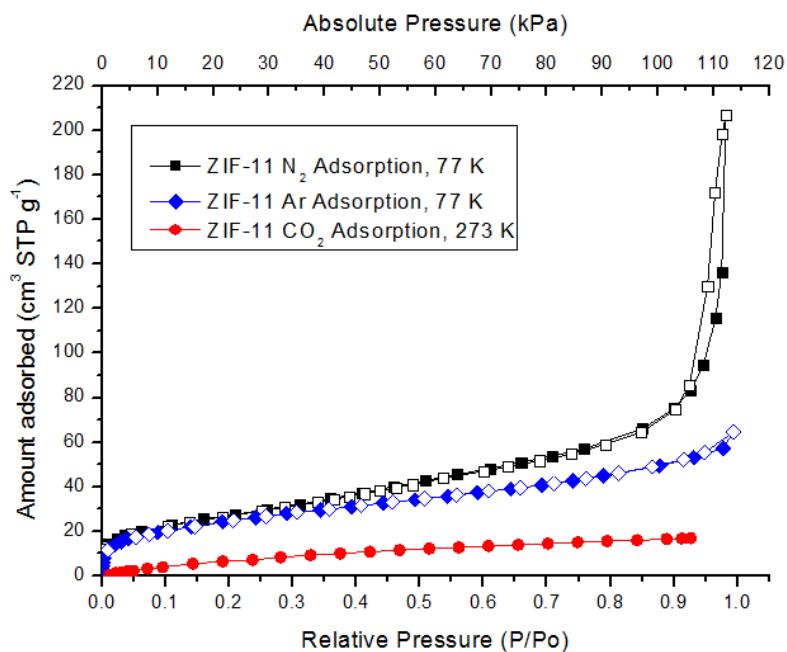


Figure 5. Adsorption isotherms of N₂ at 77K, Ar at 77 K and CO₂ at 273 K on ZIF-11. Relative pressure refers to N₂ and Ar while the absolute pressure axis refers to the CO₂ isotherm. Open symbols indicate desorption points.

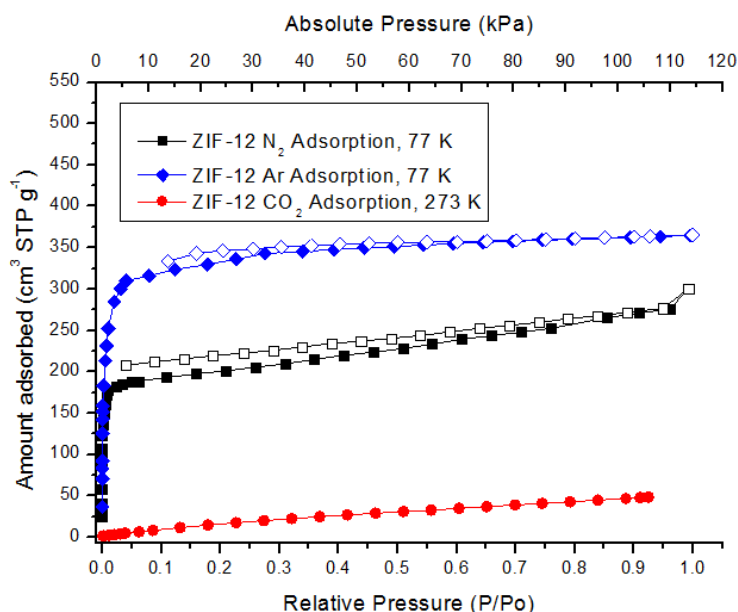


Figure 6. Adsorption isotherms of N₂ at 77 K, Ar at 77 K and CO₂ at 273 K on ZIF-12. Relative pressure refers to N₂ and Ar while the absolute pressure axis refers to the CO₂ isotherm. Open symbols indicate desorption points.

The CO₂ adsorption isotherms of both ZIF-7 and ZIF-9 (Figures 3 and 4) show a sudden CO₂ uptake between 10 and 20 kPa. ZIF-7 and ZIF-9 both show hysteresis in their desorption isotherms, and a step that is compatible with a sorbate-induced gate-opening phenomenon, a feature that has been widely reported in the literature (13, 14, 20, 33). Regarding the N₂ or Ar isotherms of ZIF-7 and ZIF-9 in Figs 3 and 4 (both with similar structural dimensions (5)), these barely show any adsorption, which can be due to the gases' high kinetic diameters (0.364 and 0.354 nm respectively, for N₂ and Ar) (31) compared to their pore window size (0.29 nm) (7). CO₂, however, (which has a kinetic diameter of 0.330 nm (31)) has been shown to be admitted into the framework. It has been shown that ZIF-7 can selectively separate ethane over ethylene (21), which have even bigger kinetic diameters (0.4163 and 0.4443 nm for ethylene and ethane, respectively (34)), with both molecules inducing phase changes in the structure at

different pressures. This indicates the ability of ZIF-7 to adsorb molecules with higher kinetic diameters, due to the existence of specific interactions present between ethane/ethylene and the ZIF-7 structure. Based on the results presented in Figure 3, these interactions do not seem to be present in N₂ and Ar, as adsorption of these gases does not induce a phase change.

Figures 3, 4, and 6 show that ZIF-7, ZIF-9, and ZIF-12 exhibit a similar maximum CO₂ adsorption capacities, with ZIF-7 showing 51 cm³ STP g⁻¹ at approximately 105 kPa, followed by ZIF-12 with 48 cm³ STP g⁻¹ and ZIF-9 with 44 cm³ STP g⁻¹ at 105 and 120 kPa, respectively. These results indicate very similar CO₂ adsorption capacities when compared to other ZIFs with GME topology (ZIF-68, ZIF-69, ZIF-81 and ZIF-82) (9, 35). The results in Figure 4 also show the step associated with a phase change of the ZIF-9 framework structure. The only difference between ZIF-7 and ZIF-9 is the metal centre, which suggests a similar mechanism for this phase change, that is, a gate-opening effect upon adsorption of guest molecules. As seen for ZIF-7, this gate-opening is consistent with a rotation of the benzimidazole linkers which increases the diameter of the cavities and allows for increased adsorption of CO₂. A recent study by Cuadrado-Collados et al. (36) highlighted the importance of complete solvent removal and equilibration times, and showed CO₂ to be less sensitive to the blocking effect of DMF. In that paper, nitrogen was shown to be adsorbed by ZIF-7 under long equilibration times of 15 days. We should note that the synthesis of ZIF-7, ZIF-9 and ZIF-11 was carried out with ethanol, and ZIF-12 was synthesised with methanol, and no DMF was used for the synthesis. As noted in the same paper by Cuadrado-Collados et al., an extended solvent exchange process with methanol is essential for a solvent-free structure (36).

ZIF-11 and ZIF-12 show CO₂ adsorption isotherms increasing progressively (Figures 5 and 6), indicating adsorption in the cavity that occurs without the limitation of the pore window size. The small differences in the biggest pore window are unlikely to explain the large differences seen for Ar and N₂ uptake between ZIF-11 and ZIF-12. As noted above, the differences in uptake are more likely because of the fact that ZIF-11 was exchanged with ethanol and ZIF-12 was exchanged with methanol, which, as noted by Cuadrado-Collados et al. (36), is essential for obtaining a solvent-free structure. Our results further confirm this observation. In addition, these ZIFs, despite having the same topology and similar pore size apertures, present different N₂, Ar and CO₂ adsorption isotherms in terms of capacity and shape. Again, some care should be taken when interpreting these results, as the structure might not be completely solvent-free and, as shown for other ZIFs, there might be specific interactions between the adsorbate molecule and the framework structure. These results reflect the influence of different solvents, as ZIF-12, which was synthesised with methanol, showed considerable uptake of Ar and N₂, whereas ZIF-11, which was synthesised with ethanol, displayed much more modest uptakes. The higher uptake of Ar in comparison with N₂ might be due to the small difference in the kinetic diameters of the gases. The kinetic diameter of Ar is 0.354 nm and the kinetic diameter of N₂ is 0.364 nm, meaning that the difference is only 0.01 nm. However, given that the largest pore window of ZIF-12 is 0.32, such a small difference might be enough to explain the higher uptakes of Ar in comparison with N₂.

ZIF-11 and ZIF-12 have a difference of 0.02 nm in their biggest pore window diameter (eight- vs six- membered rings, 0.30 and 0.32 nm, respectively), which allows them to

adsorb N₂ and Ar (0.364 and 0.354 nm). These results indicate that ZIF-11 and ZIF-12 might also possess flexible structures, as seen in ZIF-7 and ZIF-9. The fact that ZIF-11 and ZIF-12 have slightly larger pore sizes than ZIF-7 (0.30 and 0.32 vs 0.29 nm) suggests that the pore windows of ZIF-11 and ZIF-12 can stretch under no/low electrostatic interactions to adsorb N₂ and Ar. The difference between the pore size of ZIF-7 and CO₂ is 0.04 nm, whereas the difference between ZIF-11 and N₂ is 0.064 nm, meaning that ZIF-11 appears to exhibit a higher degree of pore flexibility in adsorbing the gas molecule. This possible extra flexibility is attributed to the RHO topology. The RHO topology is formed of alpha cages composed of four-, six- and eight-membered rings, (compared to the SOD, which is formed only by four- and six-membered ringed beta cages), and has two more benzimidazolate linkers on the larger pore windows to further open the pore windows of the framework.

Also, the mentioned smaller pore size and metal nature of ZIF-11 might explain some of the differences between ZIF-11 and ZIF-12 adsorption. It is also important to note that H₂ adsorption isotherms of ZIF-7 and ZIF-9 are very similar in shape and amount adsorbed (20), but the results for ZIF-11 and ZIF-12 show no hysteresis or step in the adsorption isotherm that indicate phase changes with either H₂ or with any of the gases tested in this work.

From the adsorption isotherm data, the textural properties and pore size distributions using the HK Cheng Yang DFT methodology (37, 38) have been obtained, and are shown in Supporting Information. This textural information reflects all the above-mentioned discussion, where the most relevant results are the CO₂ BET (240 and 224 m² g⁻¹) and DR micropore volumes (0.11 cm³ g⁻¹ for both using DR) of ZIF-7 and ZIF-

9. The similarity in the surface area and pore volumes indicate similar CO₂ surface adsorption capacities and accessibility of the molecules into these ZIF frameworks. Conversely, N₂ adsorption data shows ZIF-12 to have a higher BET surface area than ZIF-11 (789 and 97 m² g⁻¹ respectively) and micro- and total pore volumes (0.32 and 0.46 cm³ g⁻¹ from the DR and Gurvich methods for ZIF-12 and 0.03 and 0.30 cm³ g⁻¹ for the DR and Gurvich for ZIF-11).

4. Conclusions

Adsorption isotherms for N₂ at 77K, Ar at 77 K and CO₂ at 273 K were obtained and analysed for ZIF-7, ZIF-9, ZIF-11 and ZIF-12. ZIF-7 and ZIF-9 showed CO₂ adsorption isotherms with hysteresis and a step, corroborating sorbate-induced gate-opening phenomena as shown in the literature. While this has been studied and observed for ZIF-7, we observe the same effect for ZIF-9, which is also consistent with the rotation of the benzimidazolate linkers. This allows more CO₂ to be adsorbed in the cavities, as opposed to Ar and N₂, which showed no significant adsorption. ZIF-12 and ZIF-11 (RHO topology) showed uptake for N₂ and Ar, which have larger kinetic diameters than the largest pore diameter in ZIF-11 and ZIF-12, also indicating pore flexibility due to the two additional benzimidazolate linkers in its structure. The differences in uptake of Ar and N₂ in ZIF-11 and ZIF-12, which were synthesised with ethanol and methanol respectively, also show the importance of using methanol as the solvent. As noted in the literature, methanol is essential for obtaining a solvent-free structure in ZIFs, and our results further confirm this observation. The similarities in the uptake behaviours between ZIF-7 and ZIF-9 indicate the over-riding influence of topology over the metal species in determining the uptake of different gas species in these ZIFs. The marked differences in framework flexibility between ZIFs with SOD and RHO topologies may

aid in identifying other flexible zeolite topologies with similar potential to discriminate between gases of similar molecular size for applications in gas separation.

5. Acknowledgements

The authors thank the University of Bath for a URS studentship for AND and a Prize Research Fellowship for VPT, the support from the UK Engineering and Physical Sciences Research Council (EPSRC) for VPT (EP/R01650X/1) and the SUPERGEN H2FC grant EP/J016454/1, which funded most of this work. NB acknowledges funding from the EPSRC, grant code EP/K021109/1. KS and JVR acknowledge support and funding from ANPCyT, CONICET and UNSL.

6. Supporting information

Thermogravimetric analysis, adsorption and desorption data, surface area and the pore size distributions for all of the materials are included in the Supporting Information.

7. References

1. Lim KL, Kazemian H, Yaakob Z and Daud WRW. Solid-state Materials and Methods for Hydrogen Storage: A Critical Review. *Chem Eng Technol* **33**(2):213-26 (2010).
2. Rowsell JLC and Yaghi OM. Strategies for hydrogen storage in metal-organic frameworks. *Angew Chem Int Edit* **44**(30):4670-9 (2005).
3. Durbin DJ and Malardier-Jugroot C. Review of hydrogen storage techniques for on board vehicle applications. *Int J Hydrogen Energ* **38**(34):14595-617 (2013).
4. Zuttel A. Hydrogen storage methods. *Naturwissenschaften* **91**(4):157-72 (2004).
5. Park KS, Ni Z, Cote AP, Choi JY, Huang RD, Uribe-Romo FJ, et al. Exceptional chemical and thermal stability of zeolitic imidazolate frameworks. *P Natl Acad Sci USA* **103**(27):10186-91 (2006).
6. Phan A, Doonan CJ, Uribe-Romo FJ, Knobler CB, O'Keeffe M and Yaghi OM. Synthesis, Structure, and Carbon Dioxide Capture Properties of Zeolitic Imidazolate Frameworks. *Accounts Chem Res* **43**(1):58-67 (2010).
7. He M, Yao JF, Liu Q, Zhong ZX and Wang HT. Toluene-assisted synthesis of RHO-type zeolitic imidazolate frameworks: synthesis and formation mechanism of ZIF-11 and ZIF-12. *Dalton Trans* **42**(47):16608-13 (2013).

8. Biswal BP, Panda T and Banerjee R. Solution mediated phase transformation (RHO to SOD) in porous Co-imidazolate based zeolitic frameworks with high water stability. *Chem Commun* **48**(97):11868-70 (2012).
9. Banerjee R, Phan A, Wang B, Knobler C, Furukawa H, O'Keeffe M, et al. High-throughput synthesis of zeolitic imidazolate frameworks and application to CO₂ capture. *Science* **319**(5865):939-43 (2008).
10. Ruthven DM. *Principles of adsorption and adsorption processes* Wiley, New York ; Chichester. (1984).
11. Gaillac R, Pullumbi P, Beyer KA, Chapman KW, Keen DA, Bennett TD, et al. Liquid metal-organic frameworks. *Nat Mater* **16**(11):1149-55 (2017).
12. Fairen-Jimenez D, Moggach SA, Wharmby MT, Wright PA, Parsons S and Duren T. Opening the Gate: Framework Flexibility in ZIF-8 Explored by Experiments and Simulations. *J Am Chem Soc* **133**(23):8900-2 (2011).
13. Aguado S, Bergeret G, Titus MP, Moizan V, Nieto-Draghi C, Bats N, et al. Guest-induced gate-opening of a zeolite imidazolate framework. *New J Chem* **35**(3):546-50 (2011).
14. Pera-Titus M. Intrinsic Flexibility of the Zeolitic Imidazolate Framework ZIF-7 Unveiled by CO₂ Adsorption and Hg Intrusion. *Chemphyschem* **15**(8):1581-6 (2014).
15. van den Bergh J, Gucuyener C, Pidko EA, Hensen EJ, Gascon J and Kapteijn F. Understanding the anomalous alkane selectivity of ZIF-7 in the separation of light alkane/alkene mixtures. *Chem Eur J* **17**(32):8832-40 (2011).
16. Zhao P, Lampronti GI, Lloyd GO, Suard E and Redfern SAT. Direct visualisation of carbon dioxide adsorption in gate-opening zeolitic imidazolate framework ZIF-7. *J Mater Chem A* **2**(3):620-3 (2014).
17. Arami-Niya A, Birkett G, Zhu ZH and Rufford TE. Gate opening effect of zeolitic imidazolate framework ZIF-7 for adsorption of CH₄ and CO₂ from N₂. *J Mater Chem A* **5**(40):21389-99 (2017).
18. Zhao P, Lampronti GI, Lloyd GO, Wharmby MT, Facq S, Cheetham AK, et al. Phase Transitions in Zeolitic Imidazolate Framework 7: The Importance of Framework Flexibility and Guest-Induced Instability. *Chem Mater* **26**(5):1767-9 (2014).
19. Du Y, Wooler B, Nines M, Kortunov P, Paur CS, Zengel J, et al. New High- and Low-Temperature Phase Changes of ZIF-7: Elucidation and Prediction of the Thermodynamics of Transitions. *J Am Chem Soc* **137**(42):13603-11 (2015).
20. Noguera-Diaz A, Bimbo N, Holyfield LT, Ahmet IY, Ting VP and Mays TJ. Structure-property relationships in metal-organic frameworks for hydrogen storage. *Colloid Surface A* **496**:77-85 (2016).
21. Gücüyener C, van den Bergh J, Gascon J and Kapteijn F. Ethane/Ethene Separation Turned on Its Head: Selective Ethane Adsorption on the Metal–Organic Framework ZIF-7 through a Gate-Opening Mechanism. **132**(50):17704-6 (2010).
22. Morris W, He N, Ray KG, Klonowski P, Furukawa H, Daniels IN, et al. A Combined Experimental-Computational Study on the Effect of Topology on Carbon Dioxide Adsorption in Zeolitic Imidazolate Frameworks. *J Phys Chem C* **116**(45):24084-90 (2012).
23. Schneemann A, Bon V, Schwedler I, Senkowska I, Kaskel S and Fischer RA. Flexible metal-organic frameworks. *Chem Soc Rev* **43**(16):6062-96 (2014).
24. Li Q and Kim H. Hydrogen production from NaBH₄ hydrolysis via Co-ZIF-9 catalyst. *Fuel Process Technol* **100**:43-8 (2012).
25. Thommes M, Kaneko K, Neimark AV, Olivier JP, Rodriguez-Reinoso F, Rouquerol J, et al. Physisorption of gases, with special reference to the evaluation of

surface area and pore size distribution (IUPAC Technical Report). *Pure Appl Chem* **87**(9-10):1051-69 (2015).

26. Brunauer S, Emmett PH and Teller E. Adsorption of Gases in Multimolecular Layers. *60*(2):309-19 (1938).

27. Rouquerol J, Llewellyn P and Rouquerol F. Is the BET equation applicable to microporous adsorbents? *Stud Surf Sci Catal* **160**:49-56 (2006).

28. Gurvich L. *J Phys Chem Soc Russ* **47**:49-56 (1915).

29. Dubinin MM. The Potential Theory of Adsorption of Gases and Vapors for Adsorbents with Energetically Nonuniform Surfaces. *Chem Rev* **60**(2):235-41 (1960).

30. First EL and Floudas CA. MOFomics: Computational pore characterization of metal-organic frameworks. *Microporous Mesoporous Mater* **165**:32-9 (2013).

31. Li JR, Kuppler RJ and Zhou HC. Selective gas adsorption and separation in metal-organic frameworks. *Chem Soc Rev* **38**(5):1477-504 (2009).

32. Borjigin T, Sun FX, Zhang JL, Cai K, Ren H and Zhu GS. A microporous metal-organic framework with high stability for GC separation of alcohols from water. *Chem Commun* **48**(61):7613-5 (2012).

33. Ryder MR, Civalleri B, Bennett TD, Henke S, Rudic S, Cinque G, et al. Identifying the Role of Terahertz Vibrations in Metal-Organic Frameworks: From Gate-Opening Phenomenon to Shear-Driven Structural Destabilization. *Phys Rev Lett* **113**(21) (2014).

34. Aguado S, Bergeret G, Daniel C and Farrusseng D. Absolute Molecular Sieve Separation of Ethylene/Ethane Mixtures with Silver Zeolite A. *J Am Chem Soc* **134**(36):14635-7 (2012).

35. Banerjee R, Furukawa H, Britt D, Knobler C, O'Keeffe M and Yaghi OM. Control of Pore Size and Functionality in Isoreticular Zeolitic Imidazolate Frameworks and their Carbon Dioxide Selective Capture Properties. *J Am Chem Soc* **131**(11):3875-7 (2009).

36. Cuadrado-Collados C, Fernandez-Catala J, Fauth F, Cheng YQQ, Daemen LL, Ramirez-Cuesta AJ, et al. Understanding the breathing phenomena in nano-ZIF-7 upon gas adsorption. *J Mater Chem A* **5**(39):20938-46 (2017).

37. Cheng LS and Yang RT. Improved Horvath-Kawazoe Equations Including Spherical Pore Models for Calculating Micropore Size Distribution. *Chem Eng Sci* **49**(16):2599-609 (1994).

38. Horvath G and Kawazoe K. Method for the Calculation of Effective Pore-Size Distribution in Molecular-Sieve Carbon. *J Chem Eng Jpn* **16**(6):470-5 (1983).